Journal of Superconductivity: Incorporating Novel Magnetism, Vol. 14, No. 1, 2001

Superconductivity in Mesoscopic Metal Particles

H. Boyaci,[1,3] Z. Gedik,[1] and I. O. Kulik[1,2]

Received and accepted 15 June 2000

Recently, it has been possible to construct single-electron transistors to study electronic properties, including superconductivity, in metallic grains of nanometer size. Among several theoretical results are suppression of superconductivity with decreasing grain size and parity effect, that is, dependence on the parity of the number of electrons on the grain. We study how these results are affected by degeneracy of energy levels. In addition to the time-reversal symmetry, for certain energy spectra and more generally for lattice symmetries, energy levels are strongly degenerate near the Fermi energy. For a parabolic dispersion, degeneracy d is of the order of $k_F L$, whereas the typical distance between the levels is of the order of $\epsilon_F/(k_F L)^2$ where k_F and ϵ_F are the Fermi wave vector and energy, respectively, and L is the particle size. First, using an exact solution method for BCS Hamiltonian with finite number of energy levels, we find a new feature for the well studied nondegenerate case. In that case, parity effect exhibits a minimum instead of a monotonic behavior. For d-fold degenerate states we find that the ratio of two successive parity-effect parameters Δ_p is nearly $1 + 1/d$. Our numerical solutions for the exact ground state energy of negative-U Hubbard model on a cubic cluster also give very similar results. Hence we conclude that parity effect is a general property of small Fermi systems with attractive interaction, and it is closely related to degeneracy of energy levels.

KEY WORDS: Mesoscopic systems; superconductivity; strongly correlated electrons.

1. INTRODUCTION

Recently, small metallic grains, with sizes down to 5–10 nm, became available for experimental study [1–3]. Superconducting transition in such grains manifests itself through the *parity effect*, namely, dependence of electronic properties of the grain on whether the number of electrons in the grain is even or odd. Tinkham *et al.* [1] showed that in a single-electron tunneling (SET) transistor [4] with a superconducting island, conductance channels open below a certain temperature $T^* < T_c$ only for an odd number of electrons on the superconducting grain, whereas above T^* they open symmetrically at odd and even number of electrons. This means that energy of the state with odd number of electrons shifts up by an amount Δ_p [5], so-called *parity-effect parameter*

$$\Delta_p = E_0^{(2N+1)} - \frac{1}{2}\left(E_0^{(2N)} + E_0^{(2N+2)}\right). \qquad (1)$$

Several authors [6–9] developed theories attempting to calculate properties of superconducting state of the grain with discrete electronic levels. It was assumed that the level degeneracy is totally removed, and the only parameter distinguishing the small grain from the bulk sample is the ratio of the average level spacing δ in a sample to the bulk superconducting gap Δ, δ/Δ.

There are two main motivations for studying the effect of degeneracy. First, small superconducting particles can in principle be prepared in a perfect symmetric shape [10], in which case the mesoscopic superconductivity parity effect will show novel features because of level degeneracy. The second and more important motivation is the necessity of distinguishing between the level spacing due to size effect, $\delta_1 \approx \hbar v_F/L$, and the average level spacing, $\delta_2 \approx \epsilon_F/N$, that

[1]Department of Physics, Bilkent University, Bilkent 06533, Ankara, Turkey.
[2]B. Verkin Institute for Low Temperature Physics and Engineering, Natl. Acad. Sci. of Ukraine, Kharkov 310164, Ukraine.
[3]Present Address: New York University, Psychology Department, 6 Washington Place, New York, New York 10003.

is much smaller than δ_1 (N is the total number of conduction electrons in metallic grain). The ratio δ_1/δ_2 is of the order $N^{2/3}$, which is very large for a typical mesoscopic particle of size 0.1 μm corresponding to $N \approx 10^6$. The realistic energy structure of small grain is therefore not the equidistant spectrum with level spacing δ_1, adopted in most papers on mesoscopic superconductivity, but rather peaks in the density of states with characteristic distance δ_1 accompanied by finer structure with smaller energy separation δ_2. To understand what effects such finer structure may have on superconductivity in mesoscopic particles, we adopt a model of δ_1-spaced levels with the degeneracy d (in the rest of our work we drop the index and denote level spacing by δ). Calculation of superconducting condensation energy [11] shows that energy binding per particle is *not* Δ, as may be expected from a naive picture of particle binding resulting in energy decrease 2Δ, but rather of order Δ^2/ϵ_F. Adding extra two electrons to superconductor decreases energy by 2Δ but at the same time provides a (small) shift of the chemical potential in such a way that the net energy change per particle is only $\Delta \times \Delta/\epsilon_F$. A realistic calculation of the parity effect must treat the system of interacting electrons as self-consistently as it is done in the standard BCS theory of bulk superconductors [11].

In the theory of superconductivity of Bardeen *et al.* [12], the coupling Hamiltonian is introduced in the form

$$H_{\text{int}} = g \sum_{\boldsymbol{k}\boldsymbol{k}'} c^\dagger_{\boldsymbol{k}\uparrow} c^\dagger_{-\boldsymbol{k}\downarrow} c_{-\boldsymbol{k}'\downarrow} c_{\boldsymbol{k}'\uparrow} \tag{2}$$

where operator $c^\dagger_{\boldsymbol{k}\sigma}$ creates an electron in a state with momentum $\boldsymbol{k}$ and spin projection $\sigma = \uparrow, \downarrow$. $\boldsymbol{k}$ and $-\boldsymbol{k}$ states are selected in expense of all other states (such as $\boldsymbol{k}$ and $\boldsymbol{q}$, with $\boldsymbol{q} \neq -\boldsymbol{k}$), because only these two time-reversed states lead to a singularity that results in Cooper instability, identified by logarithmic divergence of the scattering amplitude $\ln(2\hbar\omega_{\text{D}}/\epsilon)$ as $\epsilon \to 0$ [11]. Pairing of non–time-reversed states can be treated perturbatively, or can be included as a renormalization in the Fermi liquid picture.

Assume that the single electron states ψ_η in metal are decomposed as

$$\psi_\eta = \sum_{\boldsymbol{k}} a^\eta_{\boldsymbol{k}} \phi_{\boldsymbol{k}} \tag{3}$$

where $\phi_{\boldsymbol{k}}$ are plane waves. We are going to denote the time-reversal state corresponding to ψ_η by $\psi_{\bar\eta}$, which is given by the complex conjugate of ψ_η. In general, ψ_η and $\psi_{\bar\eta}$ are different states. Let us introduce the operators

$$c^\dagger_{\eta\sigma} = \sum_{\boldsymbol{k}} a^\eta_{\boldsymbol{k}} c^\dagger_{\boldsymbol{k}\sigma}. \tag{4}$$

Because $c^\dagger_{\boldsymbol{k}\sigma}$ and $c_{\boldsymbol{k}\sigma}$ obey the Fermi statistics, they are called Fermi operators. Let us consider the sum $A^\dagger = \sum_\eta c^\dagger_{\eta\uparrow} c^\dagger_{\bar\eta\downarrow}$, which can be represented as

$$A^\dagger = \sum_{\boldsymbol{k}\boldsymbol{k}'} \left(\sum_\eta a^\eta_{\boldsymbol{k}} a^{\bar\eta}_{\boldsymbol{k}'} \right) c^\dagger_{\boldsymbol{k}\uparrow} c^\dagger_{\boldsymbol{k}'\downarrow}. \tag{5}$$

If we form an interaction Hamiltonian using $A^\dagger$ and A as $\tilde H_{\text{int}} = g A^\dagger A$, $\tilde H$ contains a singular part that is identical to Eq. (2) because of the identities $a^\eta_{\boldsymbol{k}} = (a^{\bar\eta}_{-\boldsymbol{k}})^*$ and $\sum_\eta |a^\eta_{\boldsymbol{k}}|^2 = 1$ (for real ψ_η, $|\eta\sigma\rangle$ and $|\bar\eta\sigma\rangle$ turn out to be the same state and if there is no further degeneracy because of other symmetries, H_{int} reduces to the "toy model" of superconductivity that has been studied extensively in [13]). Therefore, the interaction Hamiltonian in a grain can in general be written as

$$H_{\text{int}} = g \sum_{\eta\eta'} c^\dagger_{\eta\uparrow} c^\dagger_{\bar\eta\downarrow} c_{\bar\eta'\downarrow} c_{\eta'\uparrow}. \tag{6}$$

We will further split index η into j and α, where j denotes the energy levels, and α denotes the degenerate states for this level. The only symmetry expected to hold in an irregularly shaped ultrasmall grain is the time-reversal symmetry which may lead to double degeneracy for the energy levels, for example, current carrying states. On the other hand, for certain energy spectra and more generally for lattice symmetries, energy levels are strongly degenerate near the Fermi energy. For very small particles, splitting due to weak disorder or asymmetry is much smaller than the splitting due to size effect. In this case the system can be modeled as almost degenerate, with two dimensionless parameters governing superconducting transition, namely, δ/Δ, the ratio of level spacing to bulk gap, and d, the degeneracy of split levels.

2. PARITY EFFECT FOR DEGENERATE LEVELS

In our study, for simplicity, we assume that all energy levels are d-fold degenerate and that levels are equally spaced, with level spacing being equal to δ. We start with the following pair interaction Hamiltonian that is properly modified to take the degeneracy into account

$$H = \delta \sum_{j\alpha\sigma} j c^{\dagger}_{j\alpha\sigma} c_{j\alpha\sigma} - \frac{\lambda\delta}{d} \sum_{j,j'\in S;\alpha\alpha'} c^{\dagger}_{j\alpha\uparrow} c^{\dagger}_{j\bar{\alpha}\downarrow} c_{j'\bar{\alpha}'\downarrow} c_{j'\alpha'\uparrow}, \tag{7}$$

where second sum is over the set of levels S that are lying within the $2\hbar\omega_{\mathrm{D}}$ shell centered at Fermi level, that is $j, j' \in S = \{-n_{\mathrm{c}}, \ldots, n_{\mathrm{c}}$ with n_{c} being equal to integer part of $\hbar\omega_{\mathrm{D}}/\delta$, and $\alpha = 1, \ldots, d$ runs over all the degenerate states for a given energy level. Here, $|j'\bar{\alpha}'\downarrow\rangle$ and $|j'\alpha'\uparrow\rangle$ are time-reversed states for which the matrix elements are much larger than all others [14]. For example, for a grain where eigenstates are labeled by crystal momentum $\boldsymbol{k}$, the two states are $|\boldsymbol{k}\uparrow\rangle$ and $|-\boldsymbol{k}\downarrow\rangle$. Note that there is another similar but different pair formed by $|\boldsymbol{k}\downarrow\rangle$ and $|-\boldsymbol{k}\uparrow\rangle$. In usual BCS problems, because there is a summation over $\boldsymbol{k}$, both pairs are properly taken into account. On the other hand, when we sum over energy levels rather than individual states we must be careful in including both pairs. However, the model without double degeneracy can still be used to describe the superconductivity in systems with real wave functions [13].

Next, we introduce the boson operators

$$n_{j\alpha} = \frac{1}{2}\left(c^{\dagger}_{j\alpha\uparrow} c_{j\alpha\uparrow} + c^{\dagger}_{j\bar{\alpha}\downarrow} c_{j\bar{\alpha}\downarrow}\right) \tag{8}$$

and

$$b_{j\alpha} = c_{j\bar{\alpha}\downarrow} c_{j\alpha\uparrow}. \tag{9}$$

It is easy to verify that $b^{\dagger}_{j\alpha}$ and $b_{j\alpha}$ satisfy "boson" commutation relations

$$\left[b_{j\alpha}, b^{\dagger}_{j'\alpha'}\right] = \delta_{jj'}\delta_{\alpha\alpha'}(1 - 2n_{j\alpha}). \tag{10}$$

Presence of the number operator on the right hand side is a direct consequence of the Pauli principle. With these new operators, the pairing Hamiltonian can be rewritten as

$$H = 2\delta \sum_{j\alpha} j n_{j\alpha} - \frac{\lambda\delta}{d} \sum_{j,j'\in S;\alpha\alpha'} b^{\dagger}_{j\alpha} b_{j'\alpha'}. \tag{11}$$

This Hamiltonian can be split into two parts as $H = H_{\mathrm{I}} + H_{\mathrm{eff}}$ where

$$H_{\mathrm{I}} = 2\delta \sum_{j\notin S;\alpha} j n_{j\alpha},$$

$$H_{\mathrm{eff}} = 2\delta \sum_{j\in S;\alpha} j n_{j\alpha} - \frac{\lambda\delta}{d} \sum_{j,j'\in S;\alpha,\alpha'} b^{\dagger}_{j\alpha} b_{j'\alpha'}, \tag{12}$$

and the sum in H_{I} is over noninteracting particles, whereas in H_{eff} both of the sums are over interacting particles. Interacting particles are those which occupy levels inside $2\hbar\omega_{\mathrm{D}}$ shell about the Fermi level except the singly occupied level. Because the interaction is only between pairs, this singly occupied level is removed from the set S. This is the so-called "blocking effect". As H_{I} and H_{eff} commute, eigenstates of H are products of eigenstates of H_{I} and H_{eff}, and eigenvalues of H are sums of corresponding eigenvalues of H_{I} and H_{eff}. H_{I} simply represents noninteracting particles in a potential, thus determining the ground state energy H reduces to solving for H_{eff}.

The effective Hamiltonian H_{eff} has been studied with exact diagonalization methods by Mastellone, Falci, and Fazio (MFF) [8], and by Berger and Halperin (BH) [9] for the nondegenerate case and with relatively small number of levels taken into account ($n_{\mathrm{c}} < 15$). However, there exists an exact solution for H_{eff} due to Richardson and Sherman (RS) [15]. This long-forgotten exact solution has been reintroduced to condensed matter community by Braun and von Delft [16] in the context of ultrasmall superconducting grains. Here, we briefly review the Richardson–Sherman solution. First, H_{eff} is treated without the Pauli exclusion principle, that is, hard-core Bose particles are treated as normal Bose particles. After diagonalizing that Hamiltonian for normal bosons by a canonical transformation, the following boson wave function is obtained

$$\psi_b(j_1 \ldots j_N) = \sum_p P\left\{\prod_{\boldsymbol{k}=1}^{N} \frac{1}{2\delta j_{\boldsymbol{k}} - E_{p_{\boldsymbol{k}}}}\right\}, \tag{13}$$

where N is the total number of bosons, and in $\sum_p$, P means summing over $N!$ permutations of indices $p_1, \ldots, p_N$, and the corresponding energy is

$$E = E_{p_1} + \cdots + E_{p_N}. \tag{14}$$

Next, Pauli exclusion principle is imposed with the condition that $\psi = 0$ if any two j_i are not distinct. This restriction is introduced by writing the wave function as

$$\psi(j_1 \ldots j_N) = \theta(j_1 \ldots j_N)\phi(j_1 \ldots j_N), \tag{15}$$

where $\theta(j_1 \ldots j_N)$ is equal to 1 if all j_is are distinct, and is equal to 0 otherwise. Then, after some calculation an effective Schrödinger equation for ϕ is obtained [15]

$$\begin{aligned}&(2\delta j_1 + \ldots + 2\delta j_N - E)\phi(j_1 \ldots j_N)\\ &\quad -\frac{\lambda\delta}{d}\sum_{i}^{N}\sum_{j\neq j_i}\left(1 - \sum_{k\neq i}^{N}\delta_{ik}\right)\phi\\ &\quad \times (j_1 \ldots j_{i-1}, j, j_{i+1}, \ldots j_N) = 0.\end{aligned} \tag{16}$$

For a single level which is multiple fold degenerate, ground state energy is given by

$$E_0 = 2N_\epsilon - \frac{\lambda\delta}{d}N(d - N + 1), \tag{17}$$

where d is the pair degeneracy of the level. Next, we focus on degenerate levels in the $2\hbar\omega_D$ interacting shell leading to a set of coupled equations for N pairs and M levels that are d-fold degenerate:

$$1 + 2\frac{\lambda\delta}{d}\sum_{p\neq q}^{N}\frac{1}{E_p - E_q} - \frac{\lambda\delta}{d}\sum_{\alpha}\sum_{j=-n_c}^{n_c}\frac{|2\langle n_{j\alpha}\rangle - 1|}{2\delta j - E_q} = 0, \quad q = 1, \ldots, N \tag{18}$$

where

$$E_p \neq E_q, \quad \text{for } p \neq q. \tag{19}$$

The ground state wave function is given by Eq. (13) up to a normalization constant and the corresponding ground state energy is calculated from Eq. (14).

At some values of $\lambda\delta/d$, depending upon the state under consideration, Eq. (18) has singularities. At a singularity, the restriction, given by Eq. (19), is not satisfied. However, the domain of validity of the solution can be extended by letting E_q to be complex. Complex roots E_q occur in complex conjugate pairs

$$E_{2\gamma} = x_\gamma + iy_\gamma, \quad E_{2\gamma-1} = x_\gamma - iy_\gamma, \quad \gamma = 1, \ldots, N/2, \tag{20}$$

where x_γ is real and y_γ can be either real or pure imaginary. It turns out that if N is not even, one of the roots remains real for all λ. This form of E_q preserves the reality of the ground state energy E (Eq. (14)), and also the reality of the ground state wave function [15]. At a singular point, no more than two roots can be equal, and these two equal pair energies are both $2\delta j_i$ for some j_i. The desired roots of Eq. (18) for the ground state should satisfy

$$\lim_{\lambda\to 0} E_q = 2\left(\left[\frac{q-1}{d}\right] + 1\right)\delta, \quad q = 1, \ldots, N, \tag{21}$$

that is, in the non-interacting system, the lowest N levels are occupied by N pairs, whereas levels from $N+1$ to M are unoccupied ($[\cdots]$ denotes integer part of the division). We solve Eq. (18) by a globally convergent Newton–Raphson method [17] for complex E_q (Eq. (20)) with the conditions implied by Eq. (21).

For the nondegenerate case, singularities of Eq. (18) can be removed by a suitable change of variables [18]. However it is not possible to generalize that method to a degenerate case. In this case, roots are complex for all values of λ (if N is odd, one root remains real for all λ). Figure 1 shows typical behavior of roots for the double degenerate case (see Richardson [18] for the behavior of roots in the nondegenerate case).

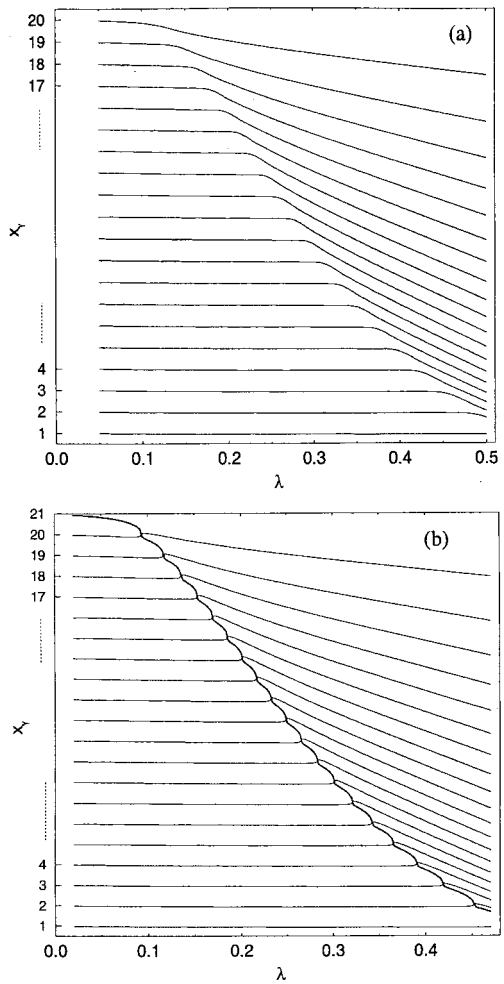

Fig. 1. Behavior of roots of Richardson–Sherman formula in the doubly degenerate case. (a) For an even number of bosons, N, all roots are complex conjugate pairs, and real parts x_γ are plotted with respect to λ. Because the roots $E_{2\gamma}$ and $E_{2\gamma-1}$ are complex conjugate pairs, their imaginary parts (y_γ) cancel each other, and the ground state energy becomes twice the sum of all x_γ; (b) When the number of bosons, N, is odd, $N-1$ roots, E_q, are complex conjugate pairs and one remaining root (E_{21}, shown by a darker solid line in (b)) is real for all λ. Again, only the real parts of roots, x_γ, are plotted with respect to λ.

The ground state energy $E_0^{(n)}$ for a given number of electrons n allows us to calculate the parity effect parameters

$$\Delta_p^{(i)} = \left| E_0^{(2n_c d+i-1)} - \frac{1}{2}\left(E_0^{(2n_c d+i-2)} + E_0^{(2n_c d+i)}\right)\right| \tag{22}$$

where $i = 1, \ldots, 2d$. Here by n we mean the number of electrons in the thin shell around the Fermi level participating in the pairing interaction. We assume that the shell is composed of n_c levels below and above the Fermi energy. Note that with this definition $E_0^{(n)}$ can take $2d$ different values and that is why i index running from 1 to $2d$ exhausts all possible values of the right hand side.

In principle, to study the effect of finite energy level spacing, we should fix the Debye frequency ω_D, which is assumed to be less affected by the boundary conditions, and change the number of levels n_c. We estimate that typical n_c values lie in the range of $\hbar\omega_D/\delta \approx 50$–$2000$, and for $\delta \approx \Delta$, we have $n_c \approx 100$. Numerical solution of Eq. (18) becomes more complicated with increasing n_c values for degenerate cases. For this reason we use an alternative approach, where we vary the Debye frequency ω_D and the coupling strength λ in order to vary δ/Δ ratio. The motivation from a physical point of view is the expectation that number parity effect, if it exists, should mainly be a function of the dimensionless parameter δ/Δ. Our numerical results support our alternative approach, as well. Given a δ/Δ ratio, if we repeat our calculations for increasing values of n_c, we observe that $\Delta_p^{(i)}/\Delta$ ratios do not change very much.

Exact diagonalization approach of MFF [8] and BH [9] for the nondegenerate case showed that both ground state properties and excitation gap are parity dependent and functions of the ratio of level spacing to the BCS gap, δ/Δ. However, systems addressed by MFF and BH are limited to relatively small number of levels, n_c, taken around Fermi level. Practically $n_c \approx 15$ is an upper limit for any exact diagonalization scheme (either Lancsoz or other methods) because of large memory space requirements. In Fig. 2 we reproduce the dependence of parity-gap parameter, $\Delta_p^{(i)}$, upon level spacing δ. Here our aim in reproducing these results, which are obtained by using much larger values of n_c (such as $n_c = 500$) for the nondegenerate case, is to compare them with those of MFF and BH. When n_c increases, we obtain a different behavior of $\Delta_p^{(1)}$ that was not observed by MFF and BH. As the number of levels n_c increases, instead of a monotonic behavior,$\Delta_p^{(1)}/\Delta$ curve exhibits a minimum at $\delta/\Delta \approx 0.5$, which cannot be observed with smaller n_c values (see Fig. 2a). On the other hand, for the dependence of $\Delta_p^{(2)}$ upon δ we observe the same behavior

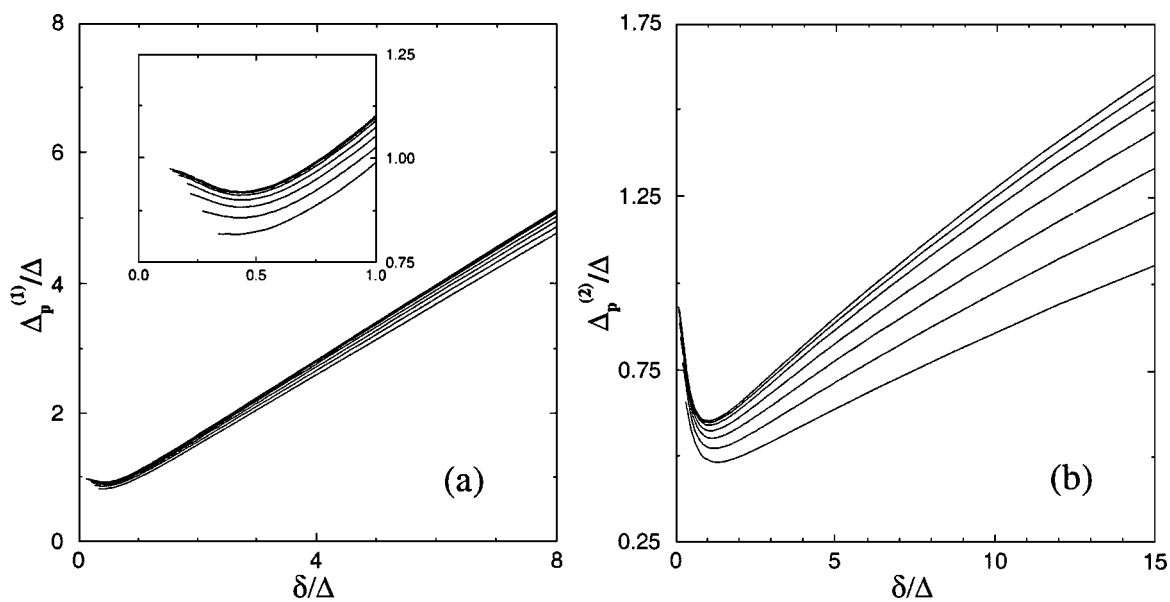

Fig. 2. Parity-effect parameters as a function of level spacing for nondegenerate case. (a) and (b) $n_c = 15$, 30, 60, 120, 240, 360, 500 from bottom to top. (a) With larger values of n_c, which are more realistic in comparison to experiments, we obtain a behavior of $\Delta_p^{(1)}$ that was not observed previously. Instead of decreasing monotonically towards $\Delta_p^{(1)}/\Delta = 1$, the curve makes a minimum at $\delta/\Delta \approx 0.5$. The inset shows the details around the minima. However, it still approaches to one after this minimum, as expected; (b) $\Delta_p^{(2)}$ has the same expected behavior as shown by many previous studies. It has a minimum at $\delta/\Delta \approx 1$, and after this minimum it turns upward towards $\Delta_p^{(2)}/\Delta = 1$.

as MFF and BH, that is, a minimum at $\delta/\Delta \approx 1$ (see Fig. 2b). Von Delft and Braun [19] show similar results for $\Delta_p^{(2)}$ in the nondegenerate case in order to compare RS exact solution to earlier approaches to the problem of mesoscopic superconductivity.

Next, we performed calculations for degenerate cases ($d \geq 2$). In Fig. 3 we present the results for doubly degenerate case ($d = 2$) which show that parity effect is still there. Similar results are obtained for higher degeneracies ($d > 2$). Some important conclusions can be drawn by comparing Figs. 2 and 3. First, $\Delta_p^{(i)}$s repeat themselves with a periodicity of two for the nondegenerate case, whereas they have a periodicity of four for the doubly degenerate case, that is, the parity-effect parameters repeat themselves with a period of $2d$. Second, one can immediately observe that there is a remarkable difference between the ratios of two different $\Delta_p^{(i)}$s for the degenerate and non-degenerate case. For example, the ratio $\Delta_p^{(1)}/\Delta_p^{(2)}$ (Fig. 2a,b) at a fixed δ/Δ value ($\approx$10), is about 5, whereas $\Delta_p^{(2)}/\Delta_p^{(3)}$ for doubly degenerate case (Fig. 3b,c) is about 1.5 for the same value of δ/Δ. We will come to a rough estimation of these values in a short while.

As it has been mentioned earlier, for certain energy spectra and more generally for lattice symmetries, energy levels are degenerate near the Fermi energy. In case of a d-fold degenerate single level with our notation $n_c = 0$, and the ground state energy (given by Eq. (17)) measured from the Fermi level is given by

$$E_0^{(n)} = \frac{\lambda\delta}{d}\left[N^2 - \left(d + \frac{1+(-1)^n}{2}\right)N\right] \qquad (23)$$

where N is the integer part of $n/2$ as above. Parity effect appears in the second term on the right hand side.

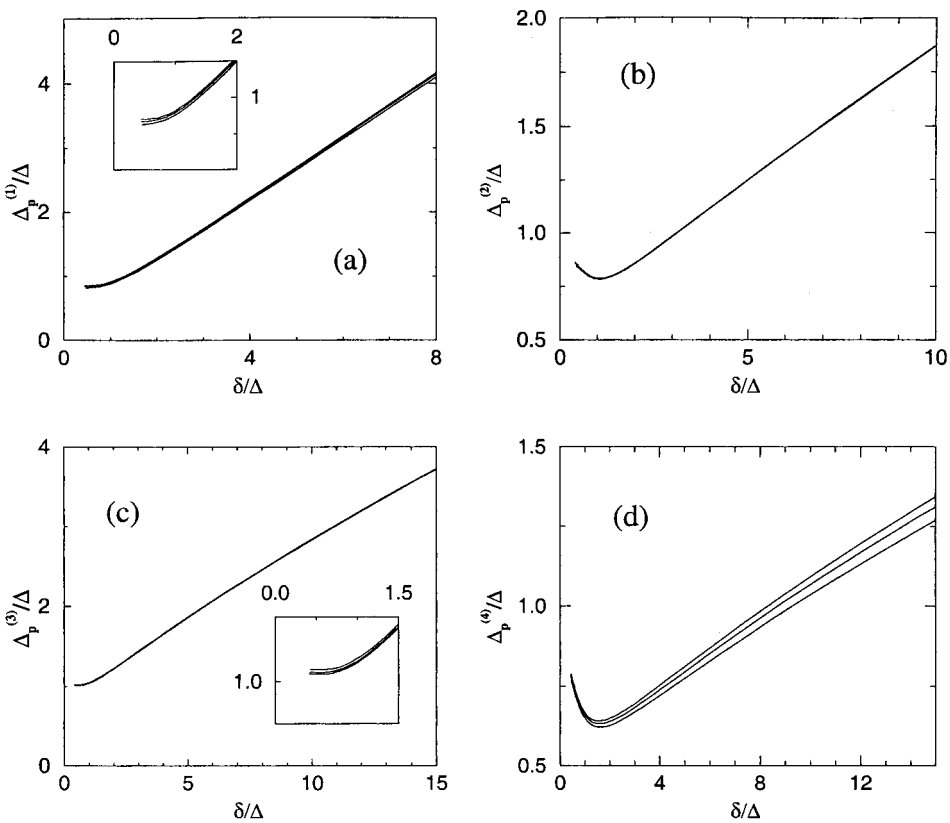

Fig. 3. Parity-effect parameters as a function of level spacing for doubly degenerate energy levels. $n_c = 20, 25, 30$ from bottom to top in (a), (b), and (d); it is from top to bottom in (c). The fact observed by comparing this figure with the one for the nondegenerate case exhibits itself when the ratios of different $\Delta_p^{(i)}$s are considered. For example, when we take ratio of $\Delta_p^{(2)}$ to $\Delta_p^{(3)}$ (compare (b) and (c)) we see that its value is much smaller than such a ratio in the nondegenerate case (compare Fig. 2a, b).

Depending upon whether n is odd or even, the factor in front of N becomes d or $d+1$, respectively. This is nothing but the blocking effect of the single electron. It is clear that when d becomes larger, this effect will become less important. By substituting Eq. (23) into Eq. (22) we obtain

$$\frac{\Delta_{\mathrm{p}}^{(\mathrm{odd})}}{\Delta_{\mathrm{p}}^{(\mathrm{even})}} = 1 + \frac{1}{d} \tag{24}$$

where odd and even superscripts stand for odd and even i in Eq. (22). Note that we consider a fixed chemical potential μ in the derivation of Eq. (24). Therefore this ratio (Eq. (24)) is valid for a parity-effect parameter $\Delta_{\mathrm{p}}^{(i)}$ for which all ground state energies, $E_0^{(n)}$, used in Eq. (22) calculated with the same chemical potential μ. Comparing Fig. 3b with Fig. 3c at $\delta/\Delta \approx 1$ we find that $\Delta_{\mathrm{p}}^{(3)}/\Delta_{\mathrm{p}}^{(2)} \approx 1.33$, which is quite close to $1 + 1/2 = 1.50$. Moreover, for $\delta/\Delta \approx 10$, we find $\Delta_{\mathrm{p}}^{(3)}/\Delta_{\mathrm{p}}^{(2)} \approx 1.51$ that is even closer to the ratio mentioned previously. For 4-fold degeneracy, where $1 + 1/d = 1.25$, we obtain similar ratios. For example $\Delta_{\mathrm{p}}^{(3)}/\Delta_{\mathrm{p}}^{(4)} \approx 1.17$ at $\delta/\Delta \approx 1$, and $\Delta_{\mathrm{p}}^{(3)}/\Delta_{\mathrm{p}}^{(4)} \approx 1.24$ at $\delta/\Delta \approx 10$. These results are not unexpected, because as δ/Δ increases, contribution of electrons at the Fermi level to the ground state energy becomes dominant, which lets single level result become a better approximation. On the other hand when μ shifts, Eq. (24) is not valid anymore and the ratio $\Delta_{\mathrm{p}}^{(\mathrm{odd})}/\Delta_{\mathrm{p}}^{(\mathrm{even})}$ becomes very different from 1. For example, $\Delta_{\mathrm{p}}^{(1)}/\Delta_{\mathrm{p}}^{(2)} \approx 5$ for nondegenerate case and $\Delta_{\mathrm{p}}^{(1)}/\Delta_{\mathrm{p}}^{(4)} \approx 5$ for doubly degenerate case at $\delta/\Delta \approx 10$.

3. PARITY EFFECT IN ATOMIC CLUSTER

We supplement the investigation of a parity effect "from above" (from macroscopic sizes down to mesoscopic sizes) by an investigation "from below", that is, starting from small clusters of atoms coupled at sites by some interaction energy [20]. Unlike Eq. (2), we choose the negative-U Hubbard interaction

$$H = -t \sum_{i \neq j} a_{i\sigma}^{\dagger} a_{j\sigma} + U \sum_{i=1}^{N} n_{i\uparrow} n_{i\downarrow} \tag{25}$$

where i and j numerate atomic sites, $a_{i\sigma}^{\dagger}$ is the creation operator at site i with spin projection σ, and $n_{i\sigma}$ is the number operator. This Hamiltonian (Eq. (25)) will reduce to a BCS Hamiltonian (Eq. (2)) in the limit of large number of sites and small U, with the difference that the interaction (Eq. (25)) is a nonretarding one, and the interaction shell (the cut-off energy) at Fermi energy is increased up to the value of the order of Fermi energy itself. In the absence of interactions for energy levels of cubic cluster, we find $-3t$, $-t$, and $3t$, where $-t$ and t are triply degenerate, and hence level spacing δ is given by $2t$. An exact solution of Hamiltonian (Eq. (25)) in a cubic cluster allowing for maximum of 16 electrons has been studied earlier [21]. The Hamiltonian matrix corresponding to Eq. (25) has a maximum dimension of $\approx 6 \times 10^4$ after reduction of the size with symmetry consideration, and ground state eigenvalue is calculated by an exact diagonalization method (of non-Lanczos type).[4] Fermi operators $a_{i\sigma}$ are represented as

$$\begin{aligned} a_{1\uparrow} &= a \otimes u \otimes u \otimes u \otimes u \cdots \otimes u \\ a_{1\downarrow} &= v \otimes a \otimes u \otimes u \otimes u \cdots \otimes u \\ a_{2\uparrow} &= v \otimes v \otimes a \otimes u \otimes u \cdots \otimes u \\ &\cdots \\ a_{8\downarrow} &= v \otimes v \otimes v \otimes v \otimes v \cdots \otimes a \end{aligned} \tag{26}$$

where a, u, v are 2×2 matrices

$$a = \begin{pmatrix} 0 & 1 \\ 0 & 0 \end{pmatrix}, \quad u = \begin{pmatrix} 1 & 0 \\ 0 & 1 \end{pmatrix}, \quad v = \begin{pmatrix} 1 & 0 \\ 0 & -1 \end{pmatrix} \tag{27}$$

and $\otimes$ is the Kronecker matrix product symbol. By changing U, we change the bulk energy gap Δ that we calculate by using BCS gap equation. For $-1 \geq U/t \geq -10$, approximating the density of states by $1/12t$, we see that the coupling parameter $\lambda \approx U/12t$ changes between 0.08 and 0.83. Therefore, at least for small $|U|$ values, we are in the weak-coupling BCS regime where an approximate solution of the gap equation can be written as $\Delta = 12t \exp(-12t/|U|)$. Nonzero parity-effect parameter, Δ_{p}, is directly seen from the energy versus electron number plot (see Fig. 4). We observe that $E_0^{(n)}$ is not a monotonic function of n. The ground state energy exhibits dips for even number of electrons. This is an unambiguous indication of the parity effect, which is a direct manifestation of Cooper pairing.

The inset in Fig. 4 shows that $\Delta_{\mathrm{p}}^{(8)} = E_0^{(7)} - (E_0^{(6)} + E_0^{(8)})/2$ is nonzero as long as there is an attractive interaction at sites, that is, $U < 0$. We find, on the contrary, that $\Delta_{\mathrm{p}} = 0$ at $U > 0$ and hence conclude

[4] A sample implementation of the method by H. Boyaci and I. O. Kulik can be found at http://www.fen.bilkent.edu.tr/boyaci/computation/eig.html.

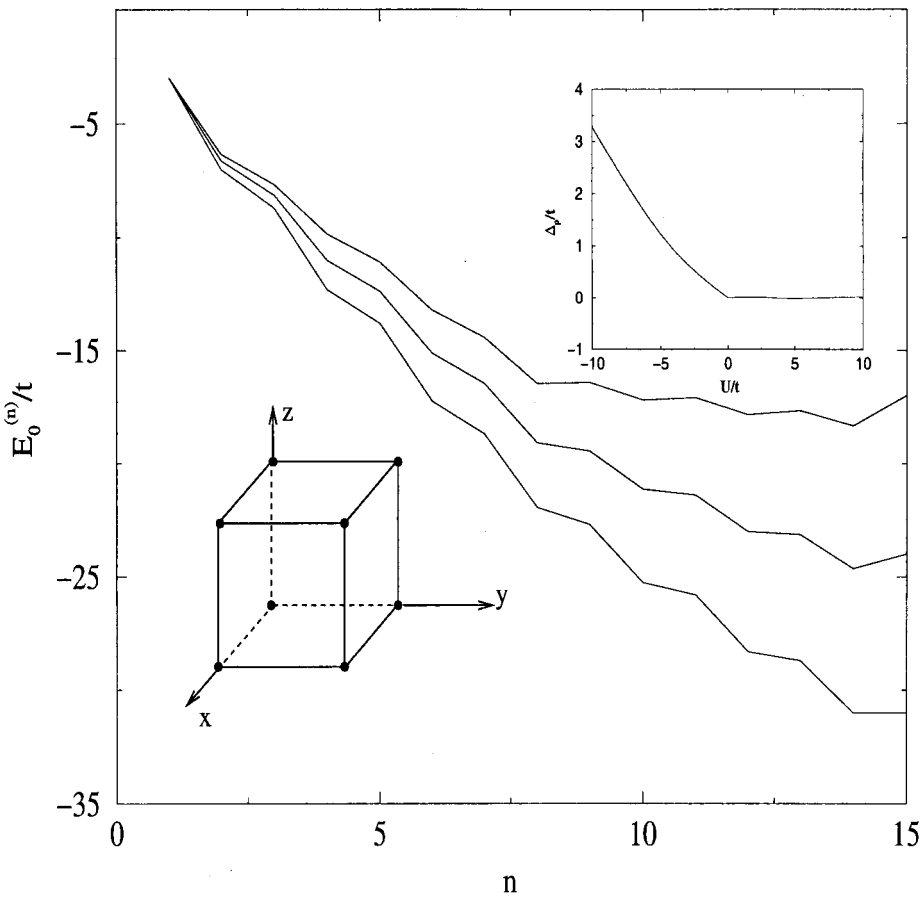

Fig. 4. Dependence of ground state energy $E_0^{(n)}$ (in units of t) upon number of particles n for $U/t = -2, -3, -4$ from top to bottom. The ground state energy exhibits drops for an even number of electrons. Lower inset shows the cubic cluster on which negative-U Hubbard model is solved. Parity effect parameter Δ_p vs. on-site interaction U at half filling is shown in the upper inset.

that repulsive Hubbard model does not lead to superconductivity. Nevertheless in principle this result does not exclude the possibility of superconductivity in a larger system with $U > 0$.

Presence of parity effect for negative-U Hubbard Hamiltonian is important, because it shows that dependence of superconducting properties on whether there are even or odd number of electrons is not specific to BCS Hamiltonian. Although our rule that the ratio of two successive parity-effect parameters is $1 + 1/d$ does not work, we clearly see that $\Delta_p^{(i)}$ values form groups in parallel to the degeneracy of levels. For example, the first line in Table I corresponds to a jump from -3 state to -1 state, whereas the next five lines correspond to energy levels -1. It is possible to understand different behaviors of $\Delta_p^{(i)}$ for $i = 3, 9$, and 15 by introducing analogue of chemical potential given by $\mu = (E_{\mathrm{HOMO}} + E_{\mathrm{LUMO}})/2$ where

Table I. $\Delta_p^{(i)} = |E_0^{(i-1)} - (E_0^{(i-2)} + E_0^{(i)})/2|$, for Different Values of i with $U = -1$[a]

i	3	4	5	6	7	8	9	10	11	12	13	14	15
$\Delta_p^{(i)}$	1.003	0.204	0.212	0.201	0.206	0.197	1.010	0.197	0.206	0.201	0.212	0.204	1.003

[a] We observe three relatively large $\Delta_p^{(i)}$ values ($i = 3, 9, 15$) corresponding to jumps between the energy levels of the cubic cluster ($-3 \to -1$, $-1 \to 1$, and $1 \to 3$).

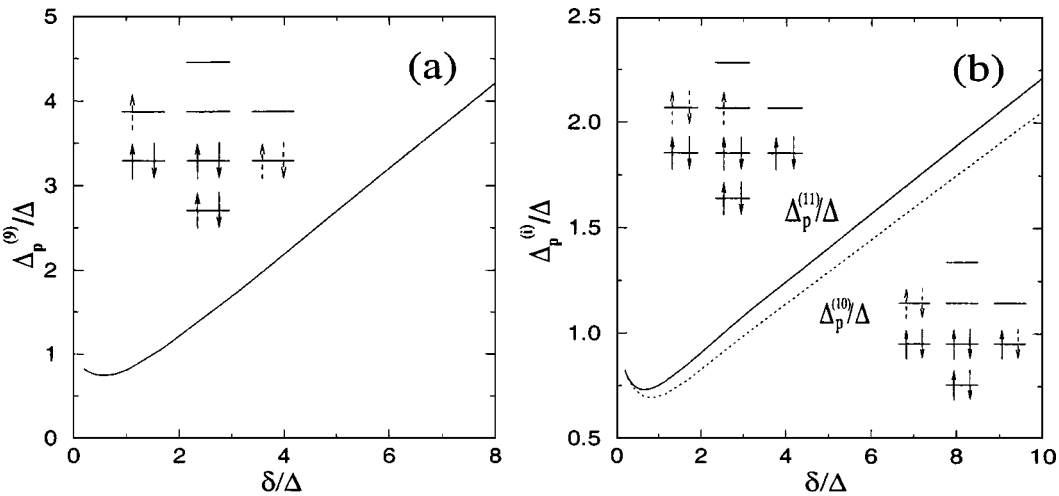

Fig. 5. Parity effect parameters $\Delta_p^{(9)}$, $\Delta_p^{(10)}$ and $\Delta_p^{(11)}$ as a function of level spacing $\delta = 2t$, for the cubic cluster where (a) $\Delta_p^{(9)} = |E_0^{(8)} - (E_0^{(7)} + E_0^{(9)})/2|$; (b) $\Delta_p^{(10)} = |E_0^{(9)} - (E_0^{(8)} + E_0^{(10)})/2|$ and $\Delta_p^{(11)} = |E_0^{(10)} - (E_0^{(9)} + E_0^{(11)})/2|$. The insets show the corresponding energy levels of the cluster. Because $\Delta_p^{(9)}$ involves the jump $-1 \rightarrow 1$, it is relatively large in comparison to $\Delta_p^{(10)}$ and $\Delta_p^{(11)}$ as can be seen in Table I.

HOMO and LUMO stand for highest occupied and lowest unoccupied molecular orbital, respectively. For $i = 3$, 9, and 15, μ is different in each $E_0^{(k)}$ value used in calculations of $\Delta_p^{(i)}$. For example, in case of $\Delta_p^{(9)} = |E_0^{(8)} - (E_0^{(7)} + E_0^{(9)})/2|$, $\mu = 0, -1$, and 1, whereas for $\Delta_p^{(11)} = |E_0^{(10)} - (E_0^{(9)} + E_0^{(11)})/2|, \mu = 1$ for all three ground states. Figure 5 shows three different parity-effect parameters, $\Delta_p^{(9)}$, $\Delta_p^{(10)}$, and $\Delta_p^{(11)}$, as a function of level spacing $\delta = 2t$. It is remarkable that the curves are very similar to those obtained for the BCS Hamiltonian. Again, because of degeneracy, $\Delta_p^{(9)}$ that involves the jump $-1 \rightarrow 1$ exhibit a slightly different behavior in comparison to $\Delta_p^{(10)}$ and $\Delta_p^{(11)}$. As far as filling of molecular orbitals is concerned, $i = 9$ case is analog of Fig. 3a, whereas $i = 10$ and 11 correspond to Fig. 3b, c, respectively.

4. CONCLUSION

In conclusion, we have studied the effect of degeneracy of discrete energy levels on the superconducting properties of a small metallic grain. We observe that parity-effect parameter, which is a measure of the dependence of energy on whether the number of electrons in the grain is even or odd, exhibits a behavior similar to the nondegenerate case for small d. We reproduced the behavior of parity-effect parameter in the well-studied non-degenerate case in order to compare our exact results with previous work. In that case the parity-effect parameter exhibits a minimum instead of a monotonic behavior. For d-fold degenerate states, it turns out that there are $2d$ different parity gaps, and furthermore, both approximate analytic solutions and exact numerical results suggest that ratio of two successive parity effect parameters is nearly $1 + 1/d$. Therefore careful measurements of parity parameters can be used to determine the degeneracy of energy levels. With increasing degeneracy, the pairing effect is suppressed. Although there is no direct evidence for existence of SET transistors with a metallic grain of perfect crystal structure, observation of perfect geometries in small grains prepared by vapor condensation technique opens a possibility for having highly symmetric structures. As we discussed previously, smallness of the average level spacing in comparison to the level spacing due to finite size effect leads to a nearly degenerate energy spectrum. Convergence of the ratio of two successive parity-effect parameters to $1 + 1/d$ as the level spacing increases can be used to detect the degeneracy.

We also show that parity effect is not specific to BCS Hamiltonian by exactly solving negative-U Hubbard model for a small atomic cluster. We can say that this is the most rigorous way to treat the problem because it does not involve any approximation like pairing assumption. Our results clearly show that parity effect exists, and hence we conclude that it is model independent and a general property of

small Fermi systems with attractive interaction. Furthermore, $\Delta_p^{(i)}/\Delta$ curves exhibit a behavior that is very similar to BCS case. Finally, grouping of $\Delta_p^{(i)}$ values according to energy levels of atomic cluster shows that degeneracy still manifests itself.

ACKNOWLEDGMENTS

This work was partially supported by the Scientific and Technical Research Council of Turkey (TUBITAK) under Grant No. TBAG 1736.

REFERENCES

1. M. Tinkham, J. M. Hergenrother, and J. G. Lu, *Phys. Rev. B* **51,** 12649 (1995).
2. C. T. Black, D. C. Ralph, and M. Tinkham, *Phys. Rev. Lett.* **76,** 688 (1996).
3. D. C. Ralph, C. T. Black, and M. Tinkham, *Phys. Rev. Lett.* **74,** 3241 (1995).
4. D. V. Averin and K. K. Likharev, in *Mesoscopic Phenomena in Solids,* B. Al'tshuler, P. Lee, and R. Webb, eds. (Elsevier, Amsterdam, 1991), p. 173.
5. K. A. Matveev and A. I. Larkin, *Phys. Rev. Lett.* **78,** 3749 (1997).
6. J. von Delft, A. D. Zaikin, D. S. Golubev, and W. Tichy, *Phys. Rev. Lett.* **77,** 3189 (1996).
7. R. A. Smith and V. Ambegaokar, *Phys. Rev. Lett.* **77,** 4962 (1996).
8. A. Mastellone, G. Falci and R. Fazio, *Phys. Rev. Lett.* **80,** 4542 (1998).
9. S. D. Berger and B. I. Halperin, *Phys. Rev. B* **58,** 5213 (1998).
10. U. Landman, talk presented at NATO-ASI Meeting, Ankara/Antalya, 1999, NATO ASI Series, Kluwer, to be published.
11. A. Abrikosov, L. P. Gorkov, I. E. Dzyaloshinsky, *Methods of Quantum Field Theory in Statistical Physics* (Dover Publications, New York, 1963).
12. J. Bardeen, L. N. Cooper, and J. R. Schrieffer, *Phys. Rev.* **108,** 1175 (1957).
13. F. Braun and J. von Delft, *Phys. Rev. B* **59,** 9527 (1999).
14. P. W. Anderson, *J. Phys. Chem. Solids* **11,** 28 (1959).
15. R. W. Richardson and N. Sherman, *Nuclear Physics* **52,** 221 (1964).
16. F. Braun and J. von Delft, *Advances in Solid State Physics* **39,** 341 (1999). Also in cond-matt/9907402.
17. W. H. Press, Saul A. Teukolsky, William T. Vetterling, and Brian P. Flannery, *Numerical Recipes in Fortran 90: The Art of Parallel Scientific Computing,* 2nd Ed. (Cambridge University Press, Cambridge, 1996).
18. R. W. Richardson, *Phys. Rev.* **141,** 949 (1966).
19. J. von Delft and F. Braun, talk presented at NATO-ASI Meeting, Ankara/Antalya, 1999, NATO ASI Series, Kluwer, to be published. Also in cond-matt/9907402.
20. E. Dagotto, *Rev. Mod. Phys.* **66,** 763 (1994).
21. H. Boyaci and I. O. Kulik, *Fiz. Nizk. Temp.* **25,** 838 (1999) [*Low Temp. Phys.* 25, 625 (1999)].